

# C 80 - 090

## Single-Mode Panel Flutter of a Wind Tunnel Flex-Wall

20009  
80001  
80006

Larry L. Erickson,\* Donald L. Kassner,† Leroy R. Guist,† and Mladin K. Chargin‡  
NASA Ames Research Center, Moffett Field, Calif.

Twice during the spring of 1978, the two steel-plate "flex-walls" that form the variable-geometry nozzle of the 11- $\times$ 11-ft transonic wind tunnel at Ames Research Center experienced a severe dynamic instability. Both walls fluttered in the fundamental beam-bending mode and experienced stresses approaching the yield strength of the material. Both flutter incidents occurred at Mach numbers of about 1.15. The tunnel, operational for 24 years, had no history of such an instability. The cause of these flutter incidents, the steps taken to prevent a recurrence, and the requalification of the facility are described.

### Nomenclature

$a$	= plate length
$D$	= plate-bending stiffness per unit width
$h$	= plate thickness
$M$	= Mach number
$N$	= number of cycles; also north
$p_{\text{atm}}$	= atmospheric pressure, taken as 76 cm Hg
$p_{\text{seal}}$	= absolute seal inflation pressure
$p_t$	= tunnel total (stagnation) pressure
$q$	= $\rho U^2 / 2$ , dynamic pressure
rpm	= revolutions per minute
$S$	= south
$\delta(\tau)$	= $(1/250) \sum_{n=1}^{250} y_0(t_n + \tau)$ , Randomdec signature <sup>2</sup>
$\zeta$	= damping from logarithmic decrement, expressed as percent of critical viscous damping
$\lambda^*$	= $2qa^3/D$ , dimensionless dynamic pressure
$\mu$	= $\rho a / \rho_m h$ , dimensionless mass ratio
$\rho$	= air density
$\rho_m$	= plate density

### I. Introduction

THE Ames 11- $\times$ 11-ft transonic wind tunnel has an operating range of  $0.4 \leq M \leq 1.4$ . Supersonic Mach numbers are obtained by a combination of rpm and nozzle-area ratio changes, the latter being produced by bending the nozzle sidewalls. Unlike most flexible-wall nozzles, the walls of the 11- $\times$ 11-ft tunnel are not supported along their length by multiple jack points. Instead, only single pairs of jacks are used at the nozzle throat to change the contraction ratio of the nozzle.

This system has been used successfully since the tunnel became operational in 1954. In the spring of 1978, however, two flex-wall flutter incidents occurred at a Mach number of about 1.15. In both cases, each of the flex-walls fluttered in its fundamental vibration mode and reached peak-to-peak displacements of about 23 cm before being stopped by emergency shutdown of the wind-tunnel compressor drive motors.

Presented as Paper 79-0797 at the AIAA/ASME/ASCE/AHS 20th Structures, Structural Dynamics, and Materials Conference, St. Louis, Mo., April 4-6, 1979; submitted May 7, 1979; revision received Dec. 11, 1979. This paper is declared a work of the U.S. Government and therefore is in the public domain.

Index categories: Nonsteady Aerodynamics; Aeroelasticity and Hydroelasticity; Structural Dynamics.

\*Research Scientist. Member AIAA.

†Aerospace Engineer.

‡Research Engineer.

The first flutter incident was initially thought to be a "once-in-twenty-four-years" shock-induced instability caused by a particular sequence of rpm changes and wall-jack settings. Consequently, continuation of tunnel operations was approved, but only after 1) an ad hoc investigation team had been formed, 2) wall accelerometers were installed, 3) a check of the walls and support structure disclosed no visible structural damage, and 4) changes were made in tunnel-operating procedures.

Ten days after the first incident, however, flutter occurred a second time. The tunnel was subsequently restricted to  $M \leq 0.90$  until the cause of the flutter was identified and corrected. The problem was finally determined to be a case of panel flutter, brought about by a loss in wall damping. Corrective measures were then taken, and the tunnel was requalified for supersonic operation in November 1978.

### II. Tunnel Description

#### Tunnel Circuit

Figure 1 is a schematic of the tunnel circuit. The notation "Aux." refers to a nearby auxiliary building containing compressors which are used to control tunnel total pressure. The tunnel is evacuated to below atmospheric pressure through valve 17; pumping to above atmospheric pressure is done through the aftercooler (radiator). To drop total pressure from an above-atmospheric condition, tunnel air is discharged to the open atmosphere through blowdown valve 23A.

#### Nozzle Configuration

A planform view of the nozzle is shown in Fig. 2. The two flex-walls are attached to the movable thrust blocks by a double row of bolts just upstream of station 00 which corresponds to the nozzle throat. The flex-walls are 3.35 m high and extend downstream to station 239 where the test section begins. (Station numbers give length in inches.) The flex-wall thickness varies in the streamwise direction.<sup>1</sup> This variation provides the proper nozzle contour when the wall is in a flexed position for supersonic flow.

A vertical T-beam is welded to each wall at station 101. The flange is pin-connected to a horizontal I-beam which is constrained to horizontal motion by pairs of rollers. This stabilizer assembly allows the flex-wall to freely bend as a wide beam, but constrains it from twisting about a streamwise axis. The flex-wall bending is produced by the jack-actuated inward motion of the thrust blocks.

Two support blocks are bolted to the underside of the thrust block. These support blocks rest on and slide across the nozzle floor, as shown in Fig. 3. This figure also shows the inflatable rubber air seal that runs along the length of the floor, ceiling, and leading edge of the nozzle wall. This seal sits in a U-

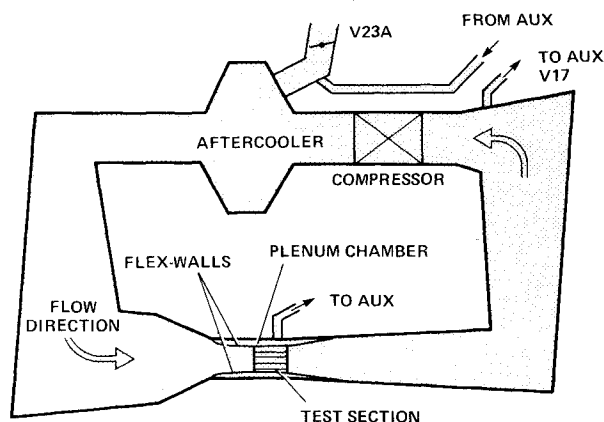


Fig. 1 Schematic of 11- x 11-ft transonic wind tunnel.

shaped Teflon boot and is held in place by Z-clips bolted to the vertical nozzle wall. During tunnel operations, the seals are kept inflated, except when the wall jacks are moving the thrust blocks. When the jacks start, the seals are automatically vented to atmospheric pressure; when the jacks stop, the seals are automatically inflated.

### III. Test Conditions at Time of Flutter Incidents

#### First Flutter Incident: April 20, 1978

This incident occurred after a series of angle-of-attack conditions had been completed at  $M=1.10$ . After returning the model to  $\alpha=0$  deg, the wind-tunnel operator started the procedure to increase Mach number to 1.20 and to lower total pressure. With the jacks forcing the thrust blocks toward the tunnel centerline and the compressor rpm changing, flutter occurred almost immediately after beginning the pressure blowdown adjustments. The flutter was made evident to the test crew by "a rather violent control-room vibration coupled with a noticeable resonant sound." A fast stop was initiated, cutting power to the compressor drive motors, and the flutter ceased. The total duration of the noticeable control-room vibration was estimated to be between 5 and 10 s. Sometime during the flutter, the wall "overstress" lights came on. They are activated by mechanical feelers which sense abnormal flex-wall bending at the T-beam stabilizer.

This first flutter incident was thought to have occurred because of the particular sequence in rpm changes and in wall-jack settings coupled with a supposed tunnel "unstart," an event in which the shock jumps from its normal position downstream of the test section to an upstream position at the flex-wall. Such unstarts had occasionally occurred in the past. With a shock in the nozzle, the control-room manometer board would have shown an unusual streamwise variation in the  $\Delta p$  across the flex-wall, and the test section Mach number readout would have given a value less than 1.0. Unfortunately, due to the excitement caused by the control-room vibration (some of the test crew thought it was an earthquake) and the rush to activate a fast stop, no one observed the manometer board or the Mach number display.

Four days later (April 23, 1978), a series of checks on rpm and Mach number drifts were made at various Mach numbers up to 1.20. (This was done because of a sluggish rpm behavior noted prior to the first flutter incident.) During these checks, three separate unstarts occurred in a single attempt to reach and maintain  $M=1.10$ . There was no indication of flutter, however, and the opinion that the April 20, 1978 flutter incident was a fluke was further reinforced.

#### Second Flutter Incident: May 1, 1978

Testing of a different wind-tunnel model began on April 28, 1978. The first test point of the fifth run was to be at  $M=1.4$ ,  $p_t=75.0$  cm Hg, but flutter occurred before this condition was reached. Again, the flutter produced shaking and rumbling in the control room and activated the overstress lights.

Just after the initiation of a fast stop action, one of the test personnel noticed that the Mach number read 1.13 and the rpm was dropping. The Mach number readout is updated at 3-s intervals, which strongly suggests, but does not conclusively prove, that the flow in the test section was still supersonic when the flex-wall flutter began. If this was true, the shock could not have been in the nozzle when the walls first began to flutter.

### IV. Flutter Motion

The flex-wall flutter left several visible traces of its motion. These, together with wall-accelerometer signals at station 101 from the second flutter incident, gave a good indication of the flutter-mode shape and frequency.

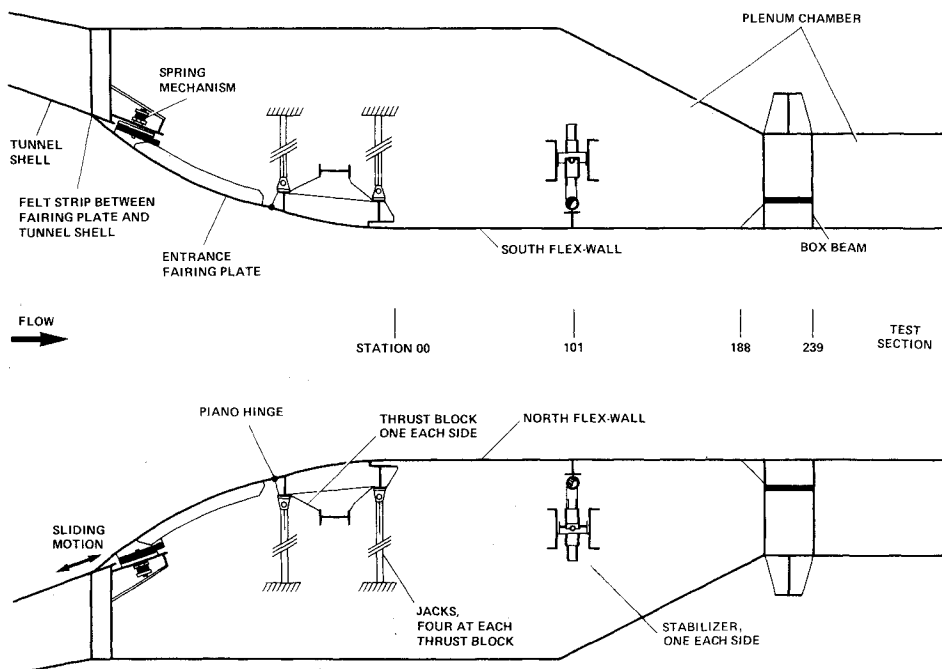


Fig. 2 Nozzle planform.

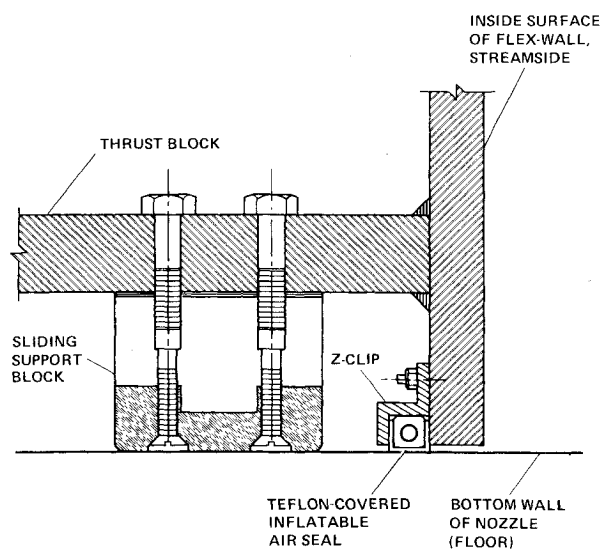


Fig. 3 Support block and inflatable seals.

#### Scuff Marks and Other Visible Evidence

The most noticeable evidence of the flex-wall flutter was the dark scuff marks made on the nozzle floor and ceiling. Figure 4 shows the south flex-wall and nozzle floor, looking upstream from inside the tunnel. In this photograph, the flex-wall is in its flat position (zero jack counts). The dark scuff-mark pattern seen on the floor, and a similar one appearing on the ceiling, were made by the inflatable seal and Teflon boot located on the opposite side of the wall, spreading out a film of dry lubricant that was between the Teflon boot and the floor/ceiling. The pattern clearly suggests that the flex-wall flutter-mode shape was similar to that of the fundamental beam-bending mode.

The flutter pattern shown in Fig. 4 is the one caused by the second flutter incident; a very similar pattern had been left by the first incident. That pattern had been partially cleaned off prior to the second flutter incident, but several short grease-pencil marks had been made on the floor to indicate its amplitude. These are also visible in Fig. 4. They show that the wall amplitude reached in the second flutter incident was slightly less than that reached in the first incident.

A fairly accurate estimate of the peak-to-peak displacement at station 101 was obtained from grease marks made by the rollers at the T-beam stabilizer assembly. A peak-to-peak displacement of 24.0 cm was obtained at the south wall, and 22.4 cm at the north wall.

#### Time History of Flutter Motion

Time histories of the north- and south-wall motion during the second flutter incident were obtained from accelerometers at station 101 and are shown in Fig. 5. The sudden growth in amplitude is quite apparent. The leveling off of this amplitude is due to the tape recorder being saturated by the accelerometer signal; therefore, it is not possible to determine whether the flutter reached a limit amplitude. Breaks in the electrical leads to both accelerometers, which occurred sometime during the flutter, presumably caused the sudden drop in signal at the end of the time history (as opposed to its being due to the flutter stopping when the compressor drive power was cut). Approximately 5 s before the end of the north-wall signal, the amplitude was increasing at a rate corresponding to a negative viscous damping ratio of  $\zeta = -3.3\%$ . The frequency at this point was about 7.5 Hz, a value nearly identical to the flex-wall fundamental bending-mode frequency in still air. In the time interval between 8 and 1 s before the end of the signal, the frequency increased from about 7.1 to 7.75 Hz. Also, notice that several small-amplitude flutter bursts took place in the interval of about 15

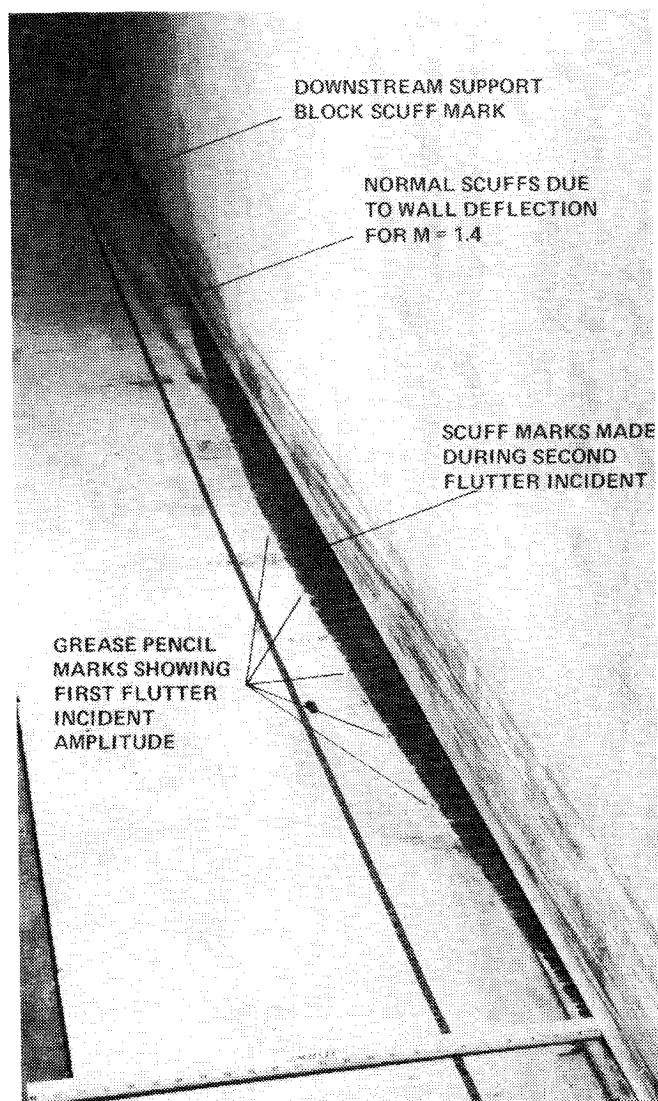


Fig. 4 South flex-wall scuff marks.

s before the final high-amplitude growth occurred. (These small bursts are not a normal wall response to the tunnel flow since they do not appear earlier in the time history.)

Figure 5 also reveals the relative phasing of the two flex-walls. Because of the way the accelerometers were oriented, the trace in Fig. 5 gives the correct phasing, that is, the walls move together and then apart, as do the tines of a struck tuning fork. This is illustrated in Fig. 6.

#### Mode Shape

Measurements of the flutter-produced scuff-mark patterns on the nozzle floor and ceiling were corrected for the seal width and the variable wall thickness to obtain estimates for the flutter-mode shape of the wall centerline (i.e., the plate middle surface). The results for the south flex-wall are shown in Fig. 7 where positive values are toward the tunnel centerline. The solid lines are for the first flutter incident and are averages of the floor and ceiling values; the solid circles indicate the station number at which the measurements were made. The measured static position curve is for wind-off with the jack setting at 1460.

The mode shape for the second flutter incident is also shown for the floor scuff marks on the tunnel side of the flex-wall. In this case, squares denote the station numbers where measurements were made.

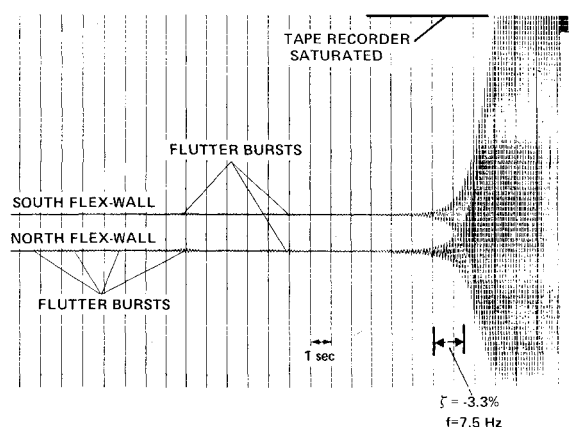


Fig. 5 Growth of flutter amplitude.

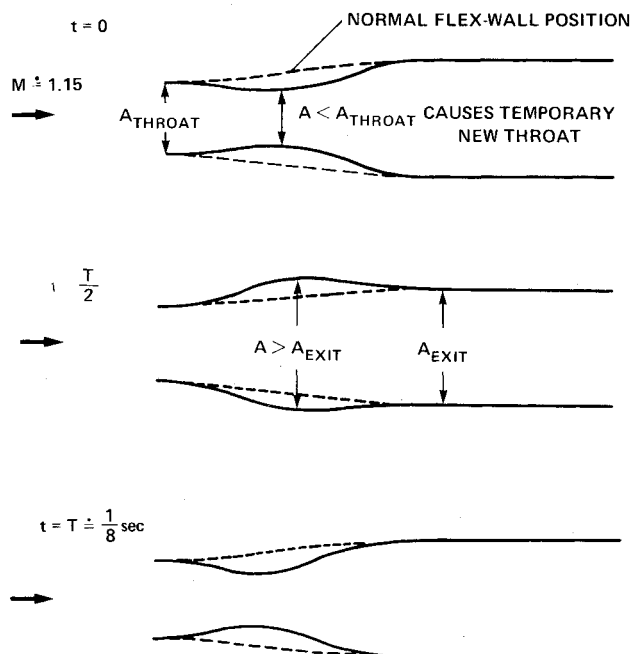


Fig. 6 Relative motion of flex-walls during second flutter incident.

To determine the resemblance between the flutter-mode shape and the fundamental free-vibration-mode shape, a NASTRAN<sup>3</sup> beam model of the flex-wall was constructed using the CBEAM element. The total mass of the flex-wall was 5528 kg including 318 kg for the stabilizer assembly.

The NASTRAN-predicted wind-off static position of the wall due to the 1460 wall-jack count is seen to be in a very good agreement with the measured position. Superimposed on this static position are the plus and minus amplitudes of the NASTRAN-predicted fundamental beam-bending mode, scaled to the 24.0-cm flutter peak-to-peak amplitude that was measured at the station 101 rollers. The resulting free-vibration-mode shape is seen to be in fairly close agreement with the measured flutter-mode shape.

### V. Wall Stress

Due to the close similarity in the measured flutter-mode shape and the NASTRAN-predicted free-vibration shape, the NASTRAN model was used to obtain an estimate of the location and value of the peak wall stress. At station 00, the static bending stress due to the south-wall 1720 (second flutter incident) jack setting was  $3.82 \times 10^7$  N/m<sup>2</sup>. Using the measured station 101 flutter amplitude of 12.0 cm, the additional bending stress at station 00 due to the first-mode vibration was  $5.27 \times 10^8$  N/m<sup>2</sup>.

### MODE SHAPES

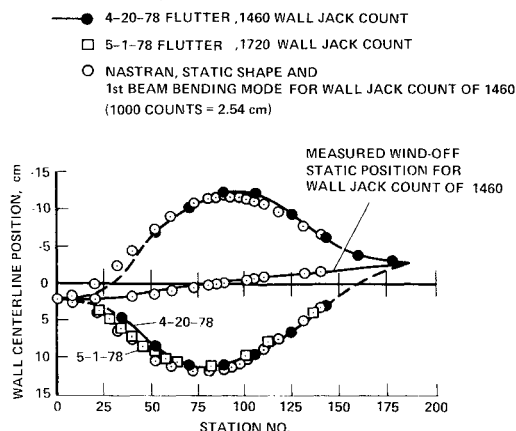


Fig. 7 South flex-wall deformation.

Although not discussed in Sec. IV, there was a 0.56-cm downstream displacement of the massive thrust block; hence, there must have been an axial load in the flex-wall. This was estimated by using the simply supported beam relation between frequency and axial load,<sup>4</sup> namely:

$$(f/f_1)^2 = 1 + (P/P_{cr})$$

where  $P$  is the axial load (positive in tension),  $P_{cr}$  is the critical buckling load,  $f$  is the fundamental beam-bending mode frequency, and  $f_1$  is the value of  $f$  at  $P=0$ . Using a value of  $f/f_1 = 1.09$ , from the discussion of Fig. 5, and the NASTRAN-predicted buckling load for clamped ends, yields  $P = 8.05 \times 10^5$  N. At station 00, the stress due to this load is  $7.58 \times 10^6$  N/m<sup>2</sup>. The total maximum stress at station 00 is then approximately  $5.72 \times 10^8$  N/m<sup>2</sup> (83,000 lb/in.<sup>2</sup>). This stress at station 00 was the highest stressed point in the flex-wall and is between 3 and 16% less than the material yield stress value obtained (from four tension-test coupons) during the tunnel fabrication period. Due to the high estimated stress at station 00, this region was inspected for cracks, using ultrasonic and magnetic particle inspection techniques. No cracks were detected.

### VI. What Caused the Flutter?

As mentioned earlier, the general opinion following the first flutter incident was that the problem was due to an unstart wherein the shock jumped from its normal position downstream of the test section to upstream positions in the nozzle. This opinion is refuted by the correlation of the events described in Sec. III (second flutter incident) with the time history of Fig. 5. The Mach number readout was at 1.13 while the control room was still noticeably shaking. Since the Mach number readout is updated every 3 s, the approximately 25-s duration of flutter activity shown in Fig. 5 establishes that the shock was downstream of the nozzle during the flutter buildup.

#### Panel Flutter

The experimental evidence discussed in Sec. IV clearly shows that the flex-wall flutter incidents were cases of first-mode, single-degree-of-freedom (SDoF) flutter, as opposed to coupled-mode flutter wherein the flutter frequency is typically about halfway between the first- and second-mode frequencies. (The NASTRAN-predicted second beam-bending-mode frequency of the flex-walls was 22.1 Hz.)

Such SDoF panel flutter is predicted theoretically.<sup>5-7</sup> Therefore, to determine if the flex-wall flutter incidents might have been cases of panel flutter, the dimensionless dynamic pressure parameter  $\lambda^* = 2qa^3/D$  was computed for the flex-walls and compared to theoretically predicted flutter values

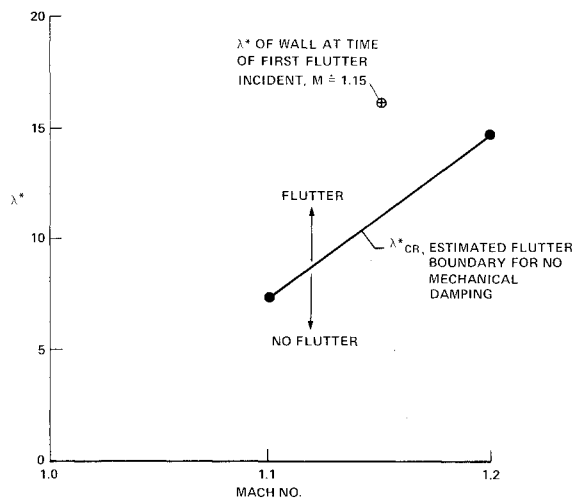


Fig. 8 Estimated flutter boundary of flex-wall,  $\mu \approx 0.016$ .

$\lambda_{cr}^*$  that were estimated from results available in the literature.<sup>6-9</sup> This comparison is presented in Fig. 8, which shows the variation in  $\lambda^*$  with Mach number. The solid line gives the theoretical flutter boundary  $\lambda_{cr}^*$  for the case of no mechanical damping; flutter occurs for  $\lambda^* > \lambda_{cr}^*$ . The flex-wall value  $\lambda_{wall}^*$ , at the time of the first flutter incident, is above the theoretical flutter boundary. Thus, even though several approximations are inherent in the results shown in Fig. 8 (see Ref. 1), the results strongly suggest that the flex-walls had been operating above the zero mechanical-damping flutter boundary for over 20 years.

Theoretical SDofF flutter boundaries at low supersonic Mach numbers and low mass ratios are very sensitive to small changes in structural damping. For example, at a mass ratio of  $\mu = 0.01$ , an increase in structural damping from  $g = 0$  to  $g = 0.05$  increases  $\lambda_{cr}^*$  for an  $a/b = 0.46$  clamped panel by factors of about 2.3 and 4.3 for  $M = 1.1$  and 1.2, respectively (Fig. 5 of Ref. 7). This then raises the question "Were there any recent changes made to the flex-walls that caused a significant loss in damping?"

#### Seal-Related Changes

The seals, which had been used for about 10 years, were replaced in January 1978. Because the new seals were ordered in the same size as those used by other Ames wind tunnels (to simplify inventory control), the width of the new seals was about 0.16 cm ( $\approx 10\%$ ) smaller than that of the old ones.

To compensate for the smaller seal width, the new seals were to have been shimmed; unfortunately, the shimming was not done. Following the second flutter incident, several Z-clips were removed from the flex-walls. There were no shims along the north flex-wall; along the south flex-wall there were 0.16-cm-thick, vertical shims, but no horizontal shims.

As shown in the next section, the lack of shims had a large effect on the friction force between the seals and the nozzle floor and ceiling. The consequent loss in flex-wall damping is believed to have caused the flutter. The restoration of damping and other safety changes made prior to the requalification of the facility for supersonic operations are also described in the following section.

### VII. Flex-Wall Characteristics and Modifications

The first part of this section describes the flex-wall friction characteristics that were measured following the second flutter incident. The second part discusses the restoration of flex-wall damping and the installation of an automatic tunnel shutdown system.

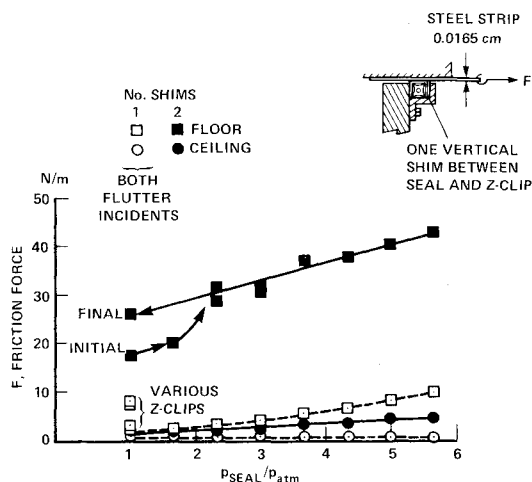


Fig. 9 Variation in friction force with seal inflation pressure; south flex-wall.

#### Post-Flutter Characteristics

Figure 9 shows the variation in south flex-wall "friction force" with seal inflation pressure. The friction force  $F$  is the force required to overcome the static friction exerted on a thin strip of steel sheet inserted between the Teflon-covered seal and the nozzle floor/ceiling, per unit width of the strip.

The open symbols give floor and ceiling results for the vertical shims that were in place during both flutter incidents. The friction force at the ceiling (open circles) is nearly zero at all pressures, indicating that the gap between the seal and ceiling is not closed by the seal inflation. At the lowest pressure, the friction force at the floor (open squares) is greater than at the ceiling and increases with inflation pressure. There is also a random variation in Z-clip height with station number. The corresponding variation in floor friction force is shown at the lowest inflation pressure.

The solid symbols in Fig. 9 show the effect of adding a 0.16-cm-thick, horizontal shim between the seal and Z-clips. There is a slight increase in friction force at the ceiling (solid circles) and a large increase at the floor (solid squares). With both the vertical and horizontal shims in place, the smaller size of the new seals is compensated for; thus, the results given by the solid symbols in Fig. 9 are probably close to what the old seals would have produced.

The sixfold or greater increase in friction force produced by the addition of the shim would be expected to produce a corresponding increase in wall damping, which was approximately  $\zeta = 2.5\%$  for the unshimmed wall with seals vented. For SDofF flutter,  $g \approx 2\zeta$ .<sup>10</sup> Thus, recalling the discussion of Fig. 8, the  $\zeta \approx 2.5\%$  damping ratio of the flex-walls with the new seals would approximately double the value of  $\lambda_{cr}^*$  at  $M = 1.1$ , still leaving  $\lambda_{wall}^*$  very near the flutter boundary. A sixfold increase in damping, however, would most probably raise  $\lambda_{cr}^*$  considerably above  $\lambda_{wall}^*$ , in which case the flex-walls would be flutter-free. So, as stated earlier, both flutter incidents were probably caused by the loss in flex-wall damping that resulted from the January 1978 seal replacement.

#### Modifications Made Prior to Facility Requalification Test

Having identified the probable cause of the flutter incidents, steps were taken to increase the flex-wall damping. This was done by shimming the seals. With the seals shimmed, there was still uncertainty about the sufficiency of the damping. Even if the former friction force had indeed been restored, it may still have been barely enough to prevent flutter. Because of this uncertainty, additional damping was provided by installing a piston damper system at the T-beam

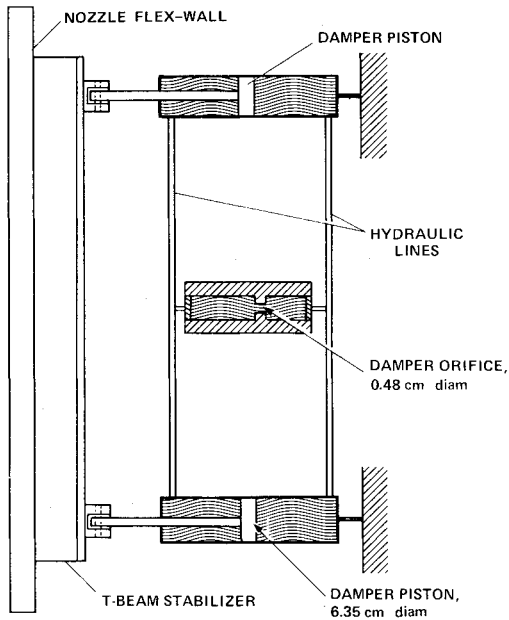


Fig. 10 Schematic of flex-wall damper system.

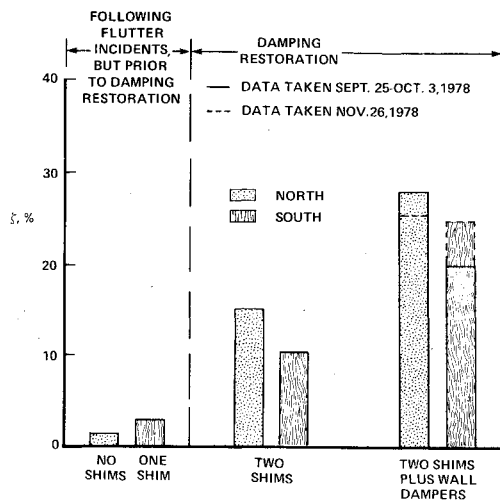


Fig. 11 Restoration of flex-wall damping.

stabilizer of each flex-wall. A schematic of this damper system is shown in Fig. 10.

To obtain the fundamental bending-mode damping of the flex-walls, a cable was attached to the stabilizer assembly at station 101 (see Fig. 2). By means of a portable, hydraulic-force generating unit, a horizontal load was applied to the cable, thus bending the flex-wall away from the tunnel centerline. The cable would break after deflecting the wall about 0.8 cm, thus producing a free decay.

The effects of the seal shims and piston dampers on the wind-off flex-wall damping are shown in Fig. 11. The first pair of results was obtained after the second flutter incident but prior to the damping restoration. The second pair shows the effect of the shims, and the third pair shows the additional effect of the wall dampers. The results given by the solid lines indicate that the shims and wall dampers provide greater damping for the north wall than the south wall. Just prior to the requalification runs on November 25-27, 1978, wall decays for the combined shims plus wall damper case were repeated. The damping for these decays is given by the dashed lines and does not repeat the earlier results, the north wall apparently having lost some damping and the south wall having gained some. The reason for the change is not known, but it is perhaps due to the cable breaking at different values

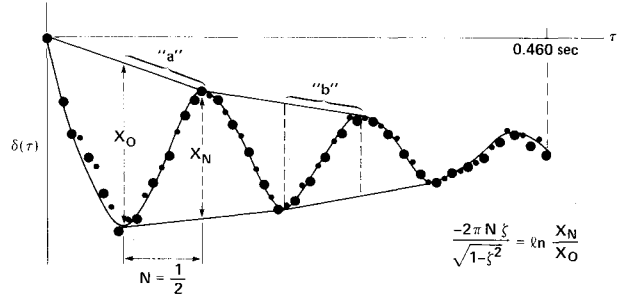


Fig. 12 Randomdec signatures of 4-15 Hz filtered strain gage signal.

of wall displacement. Departures from viscous damping behavior would then give variations in  $\zeta$ , even though the amplitude ratios were consistently taken from the same portions of the decay. (The orifice of the wall piston dampers would be expected to give a damping force approximately proportional to velocity squared, rather than to velocity to the first power, as does an ideal viscous damper.<sup>11</sup>)

As a final precaution, an automatic shutdown system was installed. As mentioned earlier, the mechanical wall overstress indicators were activated during both flutter incidents. In the second incident, this is known to have occurred before any vibration or noise was noticed in the control room. This system was subsequently modified so that in addition to the warning lights in the control room being on, buzzers would sound and the power to the compressor drives would be cut. In addition, two wall-vibration monitors were installed, one for each flex-wall. These units also cut power to the compressor drives and sound the buzzers when the wall-vibration amplitude at either of the T-beam stabilizers exceeds a preset level.

## VIII. Requalification Test

### Test Procedure and Data Reduction

Prior to going supersonic, checks were made to verify that the automatic fast-stop system worked. During separate  $M=0.6$  runs, the vibration-monitor trigger levels for the north and south walls were deliberately lowered below the ambient levels. Both monitors functioned properly and produced fast stops.

At the lowest tunnel total pressure,  $p_t/p_{atm}=0.5$  (38 cm Hg), the test continued with a Mach number sweep between 0.95 and 1.40 with the seals inflated. At that same pressure, the seals were then vented to atmospheric pressure and data were taken at  $M=1.22, 1.15$ , and 1.10. This was followed by Mach number sweeps at  $p_t/p_{atm}=1.0, 1.67$ , and 2.17 (the highest operating total pressure) with the seals still vented. Finally, at  $M=1.15$ , several wind-on wall decays were made at each of the four total pressures.

Flex-wall instrumentation consisted of strain gages near stations 00 and 101, and accelerometers at the station 101 T-beam stabilizer. Throughout the test, the strain gage and accelerometer signals were continuously recorded on magnetic tape. During fixed test conditions, a spectrum analyzer and a Randomdec computer were used to obtain on-line power spectral densities and Randomdec signatures<sup>2</sup> from the strain gage signals. Oscillograph records of wind-on wall decays were obtained from extensimeters positioned near station 101.

Although several wind-on decays of the flex-walls were made, most of the flex-wall damping estimates were obtained from the Randomdec signatures. Due to higher mode responses, the strain gage signal had to be filtered prior to computing the Randomdec signatures. Figure 12 illustrates several points concerning the data reduction. The figure actually contains two 32-point signatures obtained over two consecutive record lengths of between 15 and 30 s each. The larger circles are those of one signature; the smaller circles are

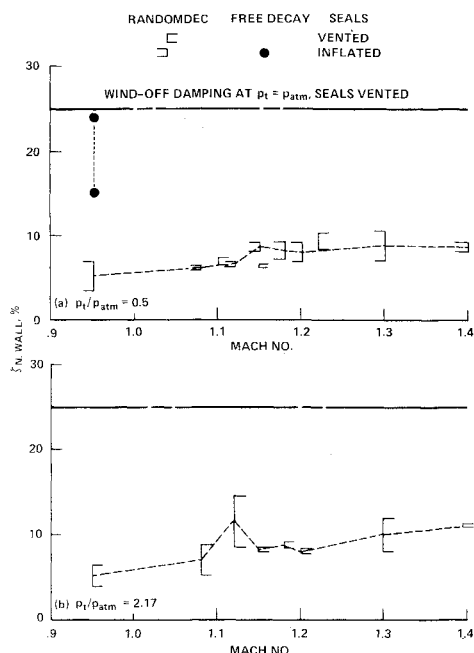


Fig. 13 Variation in north flex-wall damping with Mach number.

from the other signature. A smooth curve was hand-fitted through the points, and straight-line envelopes were drawn between consecutive peaks and valleys. Log decrements were computed over the half-cycles labeled as "a" and "b" and then expressed in terms of the damping ratio  $\zeta$  by the viscous-damping relationship shown in the figure.

#### Results and Discussion

Figure 13 shows the variation in  $\zeta$  with Mach number at two total pressures for the north flex-wall. The range in  $\zeta$  as determined from half-cycles "a" and "b" of the Randomdec signatures is given by the vertical brackets. The damping is nominally between 5 and 10% of critical, considerably below the seals-vented wind-off values shown by the horizontal lines. Similar results were obtained for the south wall.

A loss in damping at supersonic Mach numbers was expected, since single-mode panel flutter is associated with negative aerodynamic damping.<sup>5</sup> Panel flutter normally occurs only at supersonic Mach numbers, however, so the loss in damping at  $M=0.95$  is puzzling. The two solid circles in Fig. 13a give the seals-inflated segment "a" and "b" damping range at  $M=0.95$ , as obtained from a wind-on free decay, using the cable-pull technique described in Sec. VII. These results are also lower than the wind-off value.

The Randomdec signatures correspond to much smaller dynamic wall motion than that which exists during the initial portion of the cable-produced free decays. The cable usually breaks when the flex-wall has been displaced about 0.76 cm. The Randomdec signatures correspond to aerodynamic turbulence-induced wall displacements whose peak values at station 101 are only of the order of 0.05 cm or less. Comparison of the seals-vented damping, obtained from Randomdec signatures, and wind-on free decays are shown in Fig. 14 for the south wall at  $M=1.15$ . Results are given for four total pressures. Figure 14 also shows the seals-inflated damping (solid circles) at the highest and lowest total pressures, as determined from wind-on free decays.

The results of the requalification test showed that the flex-wall damping was positive over the normal tunnel-operating range at supersonic speeds, the lowest average of "a" and "b" values being  $\zeta \approx 4.4\%$ . Based on these results, the restriction of subsonic operations only was removed. In subsequent supersonic tests, there have been no flutter problems.

A final remark concerns the observation that both flutter incidents seem to have been precipitated by activating either

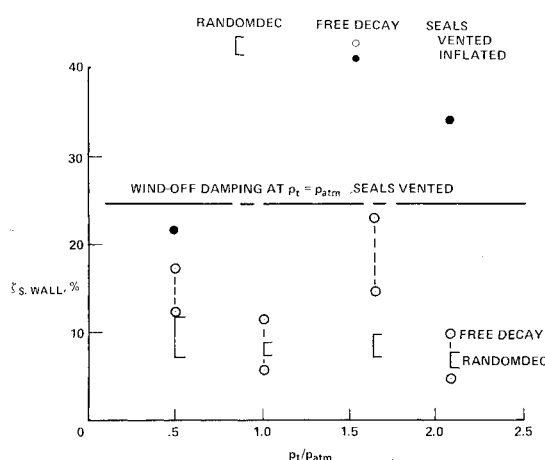


Fig. 14 Variation in flex-wall damping with total pressure at  $M=1.15$ .

the blowdown or pumpdown valves.<sup>1</sup> During the requalification test, the opening of blowdown valve 23A produced pulses in the accelerometer signals, the flex-walls apparently responding to impulses generated by the valve opening. Such impulses may have been the "perturbations" that triggered an already-unstable system.

#### IX. Concluding Remarks

The evidence indicates that the two flex-wall flutter incidents were cases of single-mode panel flutter. The flex-wall flutter boundary had apparently been outside the tunnel-operating range for over 20 years due to the damping produced by inflatable rubber air seals. When these seals were replaced with smaller seals, damping was lost, causing the flutter boundary to drop within the tunnel-operating range.

After the second flutter incident, the tunnel was restricted to subsonic operations. Subsequently, the wall damping was increased by shimming the seals and installing piston-type orifice dampers. A requalification test then cleared the tunnel for resumption of supersonic operations.

#### References

- Erickson, L.L., Kassner, D.L., Guist, L.R., and Chargin, M.K., "Investigation of Flexible Nozzle Wall Flutter Incidents in the NASA-Ames Research Center 11-x 11-Foot Transonic Wind Tunnel," AIAA Paper 79-0797, St. Louis, Mo., April 1979.
- Cole Jr., H.A., "On-Line Failure Detection and Damping Measurement of Aerospace Structures by Random Decrement Signatures," NASA CR-2205, Mar. 1973.
- McCormick, C.W., ed., "MSC/NASTRAN User's Manual," The MacNeal-Schwendler Corp., MSR-39, Los Angeles, Calif., Feb. 1978.
- Warburton, G.B., *The Dynamical Behavior of Structures*, Pergamon Press, London, England, 1964, pp. 135-137.
- Dowell, E.H., *Aeroelasticity of Plates and Shells*, Noordhoff International Publishing, Leyden, The Netherlands, 1975, pp. 21-23, 32-33.
- Dowell, E.H., "Nonlinear Oscillations of Fluttering Plate. II," *AIAA Journal*, Vol. 5, Oct. 1967, pp. 1856-1862.
- Dowell, E.H. and Voss, H.M., "Theoretical and Experimental Panel Flutter Studies in the Mach Number Range 1.0 to 5.0," *AIAA Journal*, Vol. 3, Dec. 1965, pp. 2292-2304.
- Dowell, E.H. and Voss, H.M., "Experimental and Theoretical Panel Flutter Studies in the Mach Number Range of 1.0 to 5.0," Aeronautical Systems Division, Technical Document Rept. ASD-TDR-63-449, Wright Patterson Air Force Base, Ohio, Dec. 1963.
- Erickson, L.L., "Supersonic Flutter of Flat Rectangular Orthotropic Panels Elastically Restrained against Edge Rotation," NASA TN D-3500, Aug. 1966.
- Soroka, W.W., "Note on the Relations between Viscous and Structural Damping Coefficients," *Journal of the Aeronautical Sciences*, Vol. 16, July 1949, pp. 409-410, 448.
- Creda, C.E., *Shock and Vibration Concepts in Engineering Design*, Prentice-Hall, Inc., Englewood Cliffs, N.J., 1965, pp. 7, 102-104.